Thin-film Lithium Niobate Contour-mode Resonators

Renyuan Wang and Sunil A. Bhave
School of Electrical and Computer Engineering
Cornell University
Ithaca, New York 14853, USA

Kushal Bhattacharjee
RF Micro Devices, Inc.
Greensboro, North Carolina, USA

***Abstract*—This paper presents Lithium Niobate (LN) thin-film contour mode resonators (CMR) on a piezoelectric-on-piezoelectric platform. Using this platform, we demonstrate, on a black Y136 cut Lithium Niobate thin-film, one-port high-order width extensional contour mode resonators at 463MHz and 750MHz. The electro-mechanical coupling factor (k_t^2) and quality factor (Q) of the 750 MHz resonator is 8.6% and 612, resulting in a k_t^2*Q of 53. The 463MHz resonator exhibits a k_t^2*Q of 105, with a 7% k_t^2 and 1500 Q. With this technology, we can potentially achieve multi-frequency band-pass filters with both wide bandwidth and steep roll-off.**

Keywords—contour-mode, piezoelectric, Lithium Niobate, electro-mechanical coupling factor

I. Introduction

While high-Q, narrow bandwidth "channel"-select filter arrays are actively pursued for defense applications, commercial markets demand multi-frequency "band"-select duplexer and diplexer filters, with fractional bandwidth (BW) ranging from 3% to 10%. Such filters consist of a ladder network of multiple MEMS resonators or surface-acoustic-wave resonators (Fig. 1). The achievable bandwidth of such filter is ultimately limited by the electro-mechanical coupling factor (k_t^2) of the resonators, while the roll-off is determined by resonator quality factor (Q). Therefore, resonators with both high k_t^2 and high Q are desired for large BW, steep roll-off band-pass filters.

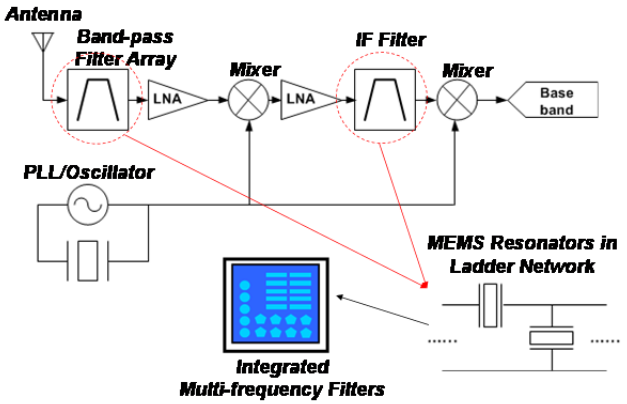

Figure 1. Conceptual schematic of a typical RF front-end in commercial wireless communication devices.

Traditional electrostatic drive MEMS resonators have shown very high quality factor [1], but suffer from extremely low k_t^2, due to the poor transduction efficiency of the electrostatic actuator. Filters using Aluminum Nitride (AlN) film bulk-acoustic-wave resonators (FBARs) have demonstrated 7% BW [2] (Fig. 2), however it is not suitable for multi-frequency integration as the resonant frequency is determined by the thickness of the AlN thin-film. On the other hand, their multi-frequency contour-mode counterparts are limited to <2.5% BW [3] due to the poor vertical-to-lateral transduction efficiency of sputtered AlN. Consequently, while FBAR filters have dominated the CDMA market, filters based on contour-mode AlN resonators have struggled to find a firm footing. Lithium Niobate based multi-frequency surface acoustic wave (SAW) filters have shown very large k_t^2 and BW [4]. But due to the 1D acoustic energy confinement in SAW configuration, energy is easily dissipated in the transverse direction as well as vertically thru the substrate, which leads to low Q and transverse parasitic modes.

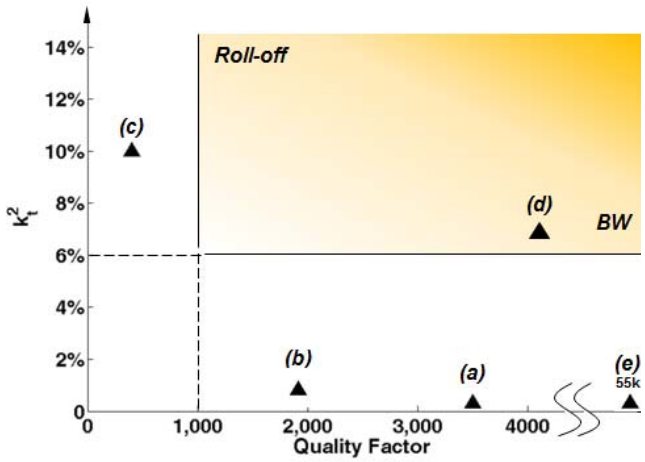

Figure 2. k_t^2 vs. Q; (a) F. Ayazi, sidewall AlN resonator; (b) G. Piazza, AlN contour-mode resonator; (c) K. Hashimoto, SAW resonator; (d) R. Ruby, AlN FBAR; (e) Nguyen, diamond disk.

Leveraging the high coupling coefficient of LN with the mode-isolation and energy trapping advantages of released and undercut mechanical structures, we present here contour mode resonators that can facilitate the development of multi-frequency, wide BW and fast roll-off filters.

II. Design of Lithium Niobate Thin-film Contour-Mode Resonators

The LN CMR consists of a block of free-standing thin-film LN with periodical inter-digitated finger transducer (IDT) on top (Fig. 3a). When a RF potential is applied to the fingers, the

electric field between the fingers generates periodic strains in the lateral direction due to the piezoelectric effect. Because of the discontinuity at the boundaries of the LN block the IDT, only certain mechanical modes of vibration can "fit in" the resonator (Fig. 3b). As a result, only an RF signal that can excite these particular modes can excite resonance in the system. The resonant frequency is expressed as

$$f = m\frac{V_{Acoustic}}{W}$$

where W is the total width of the CMR, $V_{Acoustic}$ is the Lamb wave velocity in the LN thin plate, and m is the order of the mode of vibration. Therefore, the resonant frequency of a CMR can be defined through the width of the device.

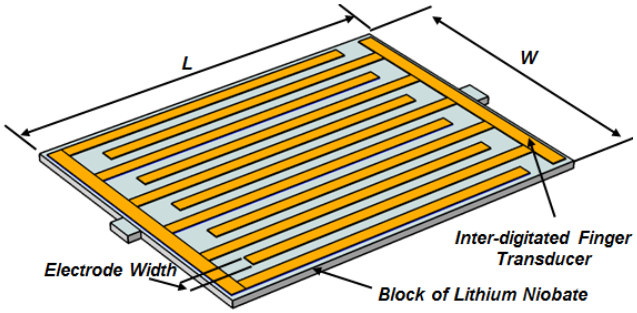

Figure 3. (a) Lithium Niobate thin-film contour-mode resonator; (b) contour plot of total displacement of S_0 Lamb mode in Y136 cut LN thin plate.

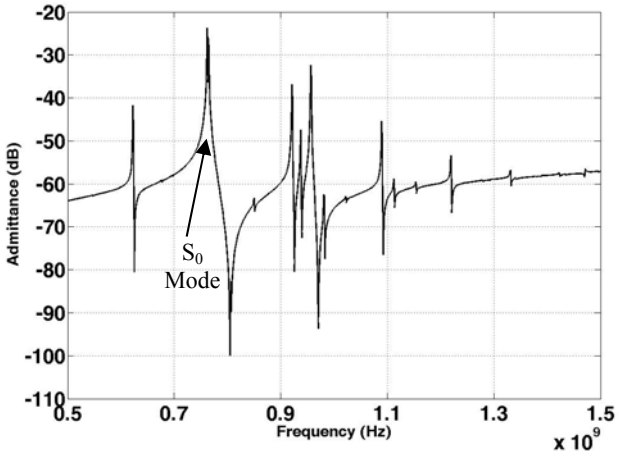

Figure 4. Simulated admittance (using COMSOL) of a 79.2um wide Lithium Niobate thin-film contour-mode resonator on Y136 cut LN thin plate.

Furthermore, the coupling factor is determined by the overlap integral between the mode shape and the excitation field profile scaled by the piezoelectric coupling coefficient. For a top nodal IDT excitation scheme on Y136 cut LN thin-film, the optimum coupling factor is achieved through the S_0 mode with wavelength of

$$\lambda = \frac{2W}{n-1}$$

where n is the total number of electrode fingers. For example, Fig. 4 shows simulated admittance of a CMR with W=79.2um and 11 electrode fingers, and 50% electrode duty cycle, where the S0 mode is resonant at 760MHz, and has a k_t^2 of ~10%.

III. FABRICATION

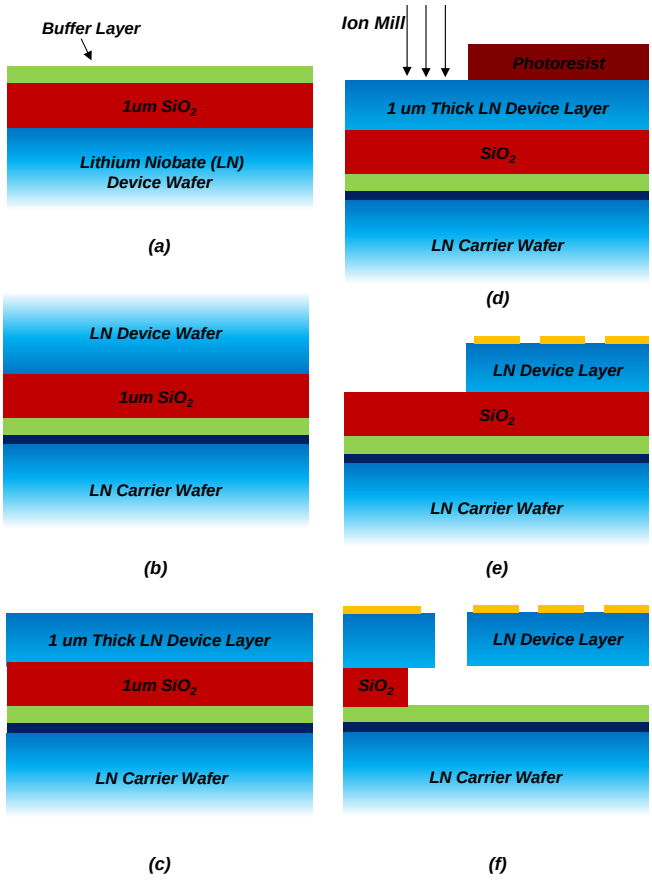

Figure 5. Fabrication process of Lithium Niobate thin-film contour mode resonators: (a) Deposition of sacrificial layer and buffer layer on device wafer; (b) Bonding of device wafer to carrier wafer; (c) Grinding the device layer to desired thickness; (d) Ion-mill defining device geometry using photoresist mask; (e) Lift-off top electrode; (f) Release device in BOE 6:1.

The semiconductor industry traditionally uses epitaxially deposited high quality thin films for the device layer. But that approach does not work well for growing high quality single crystal LN thin-films [5]. Consequently, people generally rely on thin-film transfer technology [6,7]. But the high energy ions used for slicing-off the thin-film might also degrade the thin-film surface quality. Moreover, the thin film is separated by annealing, which may cause additional problems due to thermal mismatch between the thin-film and handle wafer. Here, we use a bonding and thinning process to prepare our LN thin-film.

As shown in Fig. 5, we start with a Y136 cut LN device wafer deposited with PECVD-deposited SiO_2 sacrificial layer and a buffer layer to protect the bonding agent from BOE during release. The wafer is then flip-bonded to the LN carrier wafer using glue, and ground down to 1 um thickness. RIE etching of LN has been proposed [8-9]. However, it is very hard to achieve >80 degrees sidewall verticality using RIE due to the re-deposition of Li compound. In addition, it generally requires very high RF power and metal hard mask that is very hard to remove afterward. Therefore, ion milling is used here to define device geometry with photoresist mask. With an optimized recipe, the ion mill etching produces a sidewall slope close to 90 degrees (Fig. 6). Then, we pattern top electrode and the devices are released in buffered HF, and dried in critical point dryer.

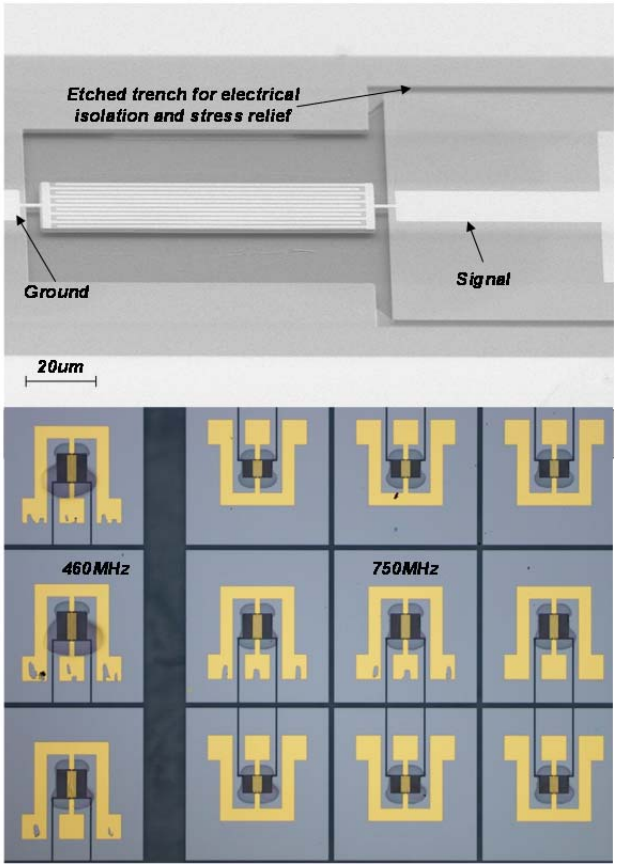

Figure 6. Top: SEM of fully released LN CMR; Bottom: microscopic photo shot of a corner of the sample showing devices with two different resonant frequencies.

In addition, the bonding and thinning process unavoidably adds stress which can build up at anchors during timed release process. Ion-milled trenches around the signal pad isolate the anchor bases, thereby providing stress relief. Fig. 6 indicates that the structure has no evidence of buckling or bowing.

IV. Experimental Result

The admittances of the CMR devices are measured using an Agilent E8364B network analyzer. The device parameters are extracted from the admittance measurement using two different methods. One is by fitting it to an mBVD model [10], the other is by using the method described in [11].

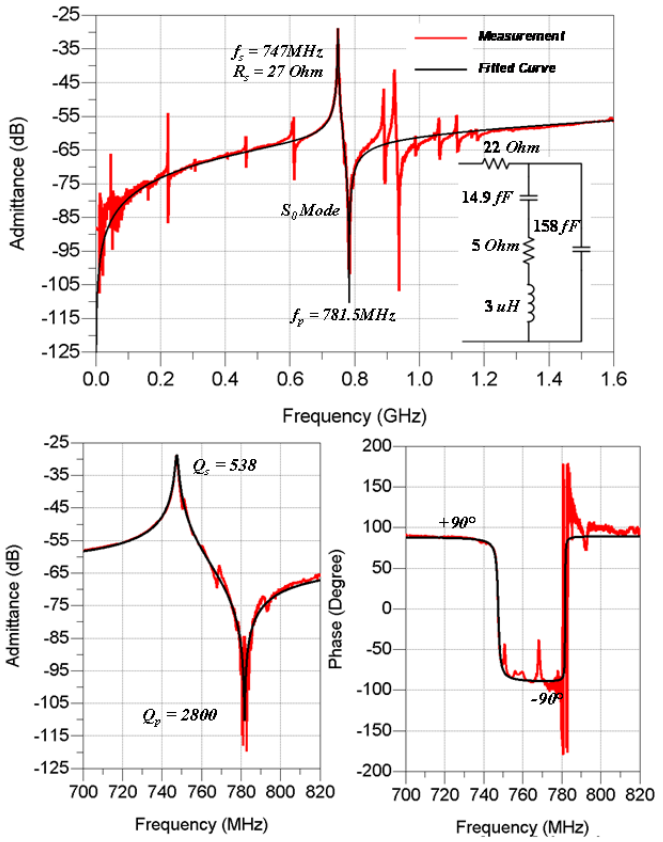

Figure 7. Top: Wide-span sweep of the admittance of the 747MHz resonator; Bottom: zoom-in view of the admittance, and phase of the admittance which shows clear transition from +90° to -90°.

Fig. 7 shows the wide-band frequency sweep and zoom-in view of a 747 MHz resonator (the same design parameters as in the simulation in section II) with the fitted curve. Calculated from the fitting parameters, the quality factors of the serial resonant (Q_s) and parallel resonant peak (Q_p) are 538 and 2800, respectively, and the impedance at series resonance is 27Ω. Using the following definition, the coupling factor is 8.6%.

$$k_t^2 = 1 - \frac{f_s^2}{f_p^2}$$

where f_s and f_p are the series and parallel resonant frequencies. It is also worth noting that the wide span admittance measurement in Fig. 7 has a very good resemblance to the COMSOL simulation (Fig. 4). In comparison, the Q_s and Q_p calculated using [11] are 612 and 3000 (Fig. 8), which matches closely to the fitted mBVD model. With a ladder configuration, such a device can enable filters at multiple frequencies with close to 9% fractional bandwidth.

Moreover, the Q_s and k_t^2 of the 463MHz resonator are 1500 and 7% (calculated using [11]). The impedance at series resonance is 51Ω (Fig. 9), and the $k_t^2 \cdot Q$ of this resonator is 105, which significantly surpasses its AlN CMR counterparts.

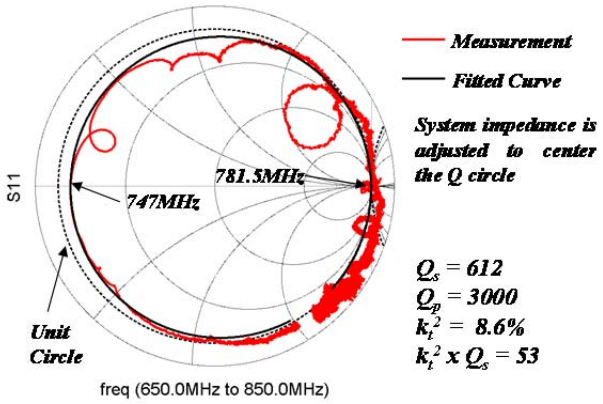

Figure 8. Quality factor calculation using the method presented in [11].

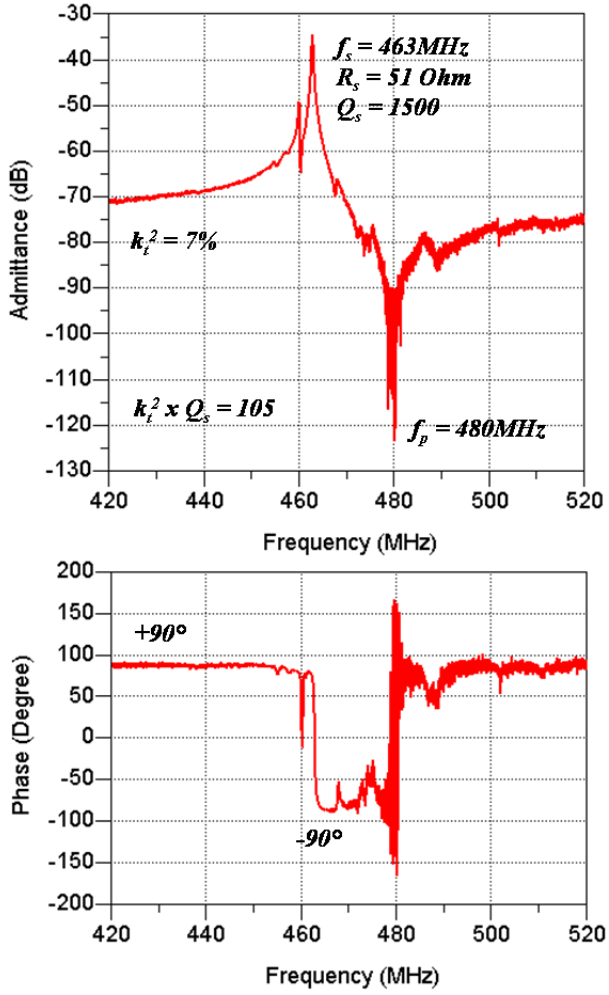

Figure 9. Measurement result of the 463MHz resonator.

V. Conclusion

LN contour mode resonators have the potential for wide band filters enabled by high $k_t^2 \cdot Q$. With a black Y136 cut Lithium Niobate piezoelectric on piezoelectric wafer, we demonstrated two resonators at 463MHz and 750MHz, with coupling factor of 7% and 8.6%, respectively. This can help realize integrated multi-frequency band-pass filters with large bandwidth and fast roll-off.

Acknowledgements

The authors wish to thank the DARPA ART program, whose generous grant has made this research possible. We would also like to thank Dr. Seungbae Lee, Professor Sheng-Shian Li, Dr. Warren Welch, and Dr. Jason Reed for initial work on LN resonator and process development.

References

[1] J. Wang, J. E. Butler, T. Feygelson, and C. T. Nguyen, "1.51-GHz nanocrystalline diamond micromechanical disk resonator with material-mismatched isolating support", *IEEE MEMS 2004*, pp. 641-644.

[2] R. Ruby, P. Bradley, J. Larson, Y. Oshmyansky, and d. Figueredo, "Ultra-miniature high-Q filters and duplexers using FBAR technology," *ISSCC 2001*, pp. 120-121

[3] G. Piazza, P. J. Stephanou, J. P. Black, R. M. White, and A. P. Pisano, "Single-chip multiple-frequency RF microresonators based on Alumium Nitride contour-mode and FBAR technologies", *Ultrasonics 2005*, 1187 (2005).

[4] M. Kadota, T. Kimura, and Y. Ida, "Ultra wide band resonator composed of grooved Cu-electrode on $LiNbO_3$ and its application to tunable filter", *Ultrasonics 2009*, pp. 2668-2671.

[5] M. Kadota, Y. Suzuki, Y. Ito, "FBAR using Lithium Niobate thin film depostied by CVD", *Ultrasonics 2010*, pp. 91-94.

[6] F. Sulser, G. Poberaj, M. Koechlin, and P. Gunter, "Photonic crystal structures in ion-sliced Lithium Niobate thin films", *Optics Express 2009*, vol. 17, no. 22, pp. 20291.

[7] S. Gong, L. Shi, G. Piazza, "High elecgtromechanical coupling MEMS resonators at 530 MHz using ion sliced x-cut $LiNbO_3$ thin film", International Microwave Symposium (2012).

[8] S. Benchabane, L. Robert, J. Rauch, A. Khelif, and V. Laude, "Highly selective electroplated Nickel mask for Lithium Niobate dry etching", *Journal of Applied Physics*, 105, 094109 (2009).

[9] S. Queste, et al., "Deep reactive ion etching of Quartz, Lithium Niobate and Lead Titanate", JNTE Proceedings, (2008).

[10] J. D. Larson, P. D. Bradley, S. Wartenberg, and R. Ruby, "Modified Butterworth-Van Dyke circuit for FBAR and automated measurement system", *Ultrasonics 2000*, pp. 863-868.

[11] D. A. Feld, R. Parker, R. Ruby, P. Bradley, and D. Shim, "After 60 years: a new formulat for computing quality factor is warranted", *Ultrasonics 2008*, pp. 431-436.